American Mineralogist, Volume 75, pages 328–344, 1990

Mixing properties of Ca-Mg-Fe-Mn garnets

R. G. Berman
Geological Survey of Canada, 588 Booth Street, Ottawa, Ontario K1A 0E4, Canada

Abstract

A model for the mixing properties of quaternary Ca-Mg-Fe-Mn garnets is developed by mathematical programming analysis of reversed phase-equilibrium data as well as calorimetric and volumetric data. The positions of end-member equilibria are established by using the thermodynamic data of Berman (1988) with minor revisions. Recent phase-equilibrium and calorimetric data strongly suggest excess entropy [5.08 J/(mol K)] on the grossular-almandine join, but considerably smaller excess enthalpy than implied by the data of Cressey et al. (1978).

Near-ideal mixing is deduced for the pyrope-almandine join from an analysis of three sets of orthopyroxene-garnet Fe-Mg exchange experiments. The derived mixing properties of Fe-Mg garnets are tested by calibrating annite properties from Ferry and Spear's (1978) experimental data on the garnet-biotite exchange equilibrium. These annite data lead to reasonable results for pressures computed from the equilibrium muscovite + almandine = annite + aluminosilicate + quartz, in contrast to results obtained with annite properties derived by using larger nonideal Fe-Mg mixing in garnet. Applications of this formulation of the garnet-biotite geothermometer yield most reasonable results when $W_{MnMg} = 0$.

Excellent support for the derived mixing properties of garnet is demonstrated by (1) convergence of different equilibria involving various garnet components in a single *P-T* region for a two-pyroxene granulite, (2) calculating pressures with the equilibrium 3 anorthite = grossular + 2 aluminosilicate + quartz that place the observed aluminosilicate polymorph in natural assemblages within its computed stability field, and (3) computing pressures as above and garnet-biotite temperatures that place rocks with more than one aluminosilicate phase in proximity to the appropriate aluminosilicate phase boundary.

Introduction

Garnet is one of the most important minerals used in petrogenetic calculations because of its occurrence in a wide range of bulk compositions over a wide range of metamorphic grades. Nevertheless, and in spite of considerable effort very little consensus has been reached about the validity of various models proposed for garnet solution properties (compare, for example, Ganguly and Saxena, 1984, with Wood, 1987). This lack of consensus stems primarily from three sources. First, experimental constraints on solution properties come from direct measurements (calorimetry, XRD) and phase-equilibrium data that make the definition of a unique set of solution properties highly sensitive to the weight given to each type of data. A related problem is the weight given to distribution-coefficient (K_D) data of natural assemblages. Second, phase-equilibrium data (or natural K_D data) cannot be used to refine solution properties independently of standard-state thermodynamic properties so that definition of the former is sensitive to the choice of the latter. Third, considerable freedom exists in selecting model complexity and calibration of model parameters because of the nonnegligible uncertainties associated with all three types of data.

Several models for quaternary Ca-Mg-Fe-Mn garnets have been proposed (Ganguly and Kennedy, 1974; Hodges and Spear, 1982; Ganguly and Saxena, 1984), although Ganguly and Saxena recommended caution in applications of their model to garnets with Fe/Mg < 3. In spite of extreme differences between the latter two models, both are still commonly used by petrologists attempting to decipher *P-T* conditions and *P-T-t* histories. Application of these and other models that apply to garnets of a limited range of compositions invariably lead to diverse results among which it is difficult for most petrologists to select objectively. The purposes of this paper are to begin to resolve these differences by showing the range of solution properties that are consistent with available experimental data and to derive a revised garnet solution model that can be applied with more confidence to a wide range of bulk compositions.

Phase-equilibrium experiments provide an important source of data from which to retrieve mixing properties, but the data derived are very sensitive to the choice of standard-state thermodynamic data used in the calculations. Recently, Berman (1988) presented a set of standard-state thermodynamic properties for 67 minerals in the system Na_2O-K_2O-CaO-MgO-FeO-Fe_2O_3-Al_2O_3-SiO_2-TiO_2-H_2O-CO_2 that were optimized using the technique

0003–004X/90/0304–0328$02.00

of mathematical programming (MAP). The internal consistency of these properties and their high degree of compatibility with available experimental data (see Berman, 1988, for supporting details) provide an excellent point of departure to derive excess free energies of the garnet solid solution. Direct measurements of mixing properties are utilized to distinguish the enthalpy, entropy, and volume contributions to the free energies of mixing.

Equations for multicomponent solutions

This study utilizes the general excess equations (Eqs. 9 and 22) derived by Berman and Brown (1984) for multicomponent solutions. For a third-degree polynomial (asymmetric excess model), the activity coefficient of the mth component is written as follows:

$$nRT \ln \gamma_m = \sum_1^p W_{i,j,k}(Q_m X_i X_j X_k / X_m - 2X_i X_j X_k), \quad (1)$$

where each W refers to $W_G = W_H - TW_S + PW_V$, Q_m is a term that counts the number of the i, j, k subscripts that are equal to m (Table 1; see also App. 1), n is the number of sites on which mixing occurs, and p is equal to the number of excess parameters needed for a given system. This number and the identity of the parameters represent all possible permutations of the three subscripts in a given component system. The major advantages of this formulation are (1) it can be memorized easily because the parameter subscripts serve as reminders of their coefficients, (2) the same equations apply to any number of components [or any degree of polynomial used to express the excess free energy if Eq. 22 of Berman and Brown (1984) is used], and (3) calculation of activity coefficients can be programmed with a minimum amount of computer code while allowing for maximum generality.

For use in systems with more than two components, a specific form of excess equation that was suggested by Wohl (1946, 1953) has found widespread use (e.g., Anderson and Lindsley, 1981; Ganguly and Saxena, 1984; Fuhrman and Lindsley, 1988; Jackson, 1989). The Wohl equation can be recast in the form of the general excess equation (i.e., Eq. 1) by substitution for the ternary $W_{i,j,k}$:

$$W_{i,j,k} = (W_{i,i,j} + W_{i,j,j} + W_{i,i,k} + W_{i,k,k} + W_{j,j,k} + W_{j,k,k})/2 - C_{i,j,k}. \quad (2)$$

Equations 1 and 2 combine to give the same equation that Anderson and Lindsley (1981) derived independently by making the ternary excess parameter a function of third-degree constants in the initial polynomial used to represent the excess free energy of solution. In the absence of ternary data to calibrate the ternary Wohl $C_{i,j,k}$ term, it can be seen that the Wohl equation approximates the ternary parameter given by Equation 1 as one-half the sum of the bounding binary parameters. This relationship has been retained in this study as experimental data are available to calibrate ternary interactions only in the Ca-Mg-Fe system.

Table 1. Q_m terms in Equation 1 for garnet excess parameters given in Table 4

Parameter	$m = 1$	$m = 2$	$m = 3$	$m = 4$
112	2	1	0	0
122	1	2	0	0
113	2	0	1	0
133	1	0	2	0
223	0	2	1	0
233	0	1	2	0
123	1	1	1	0
124	1	1	0	1
134	1	0	1	1
234	0	1	1	1

Methodology

The technique of mathematical programming (Berman et al., 1986) has been used to calibrate all relevant thermodynamic properties. Accordingly, each half-bracket on the position of a phase equilibrium is cast as an inequality constraint on the Gibbs free energy of reaction, with the directional sense of the inequality constraint reflecting from which side the equilibrium has been approached (Fig. 1). For the equilibrium

$$3\ \mathrm{An} = \mathrm{Gr} + 2\ \mathrm{Ky} + \mathrm{Qz}, \quad (A)$$

(see App. 2 for abbreviations of mineral names) these constraints are written as

$$\Delta_r G \lesseqgtr 0. \quad (3)$$

If garnet is the only phase that exhibits solid solution in the experiment, this expression can be expanded (for a site multiplicity of three) to

$$\Delta_r G^0 + 3RT \ln \gamma_{Gr} + 3RT \ln X_{Gr} \lesseqgtr 0. \quad (4)$$

Upon rearrangement, it can be seen that each experiment offers direct linear constraints on the set of Margules parameters used to represent the activity-coefficient term if the standard-state properties and X_{Gr} are known from experiment:

$$W'X' \lesseqgtr -\Delta_r G^0 - 3RT \ln X_{Gr}, \quad (5)$$

where W' represents the set of Margules parameters and X' the sum of all mole-fraction coefficients resulting from substitution of Equation 1. If any of the standard-state properties (H, S, V, C_P, α, β) are unknown or in need of refinement, these terms remain as variables on the left side of Relation 5.

The mathematical programming approach described above and discussed in more detail by Berman et al. (1986) offers several advantages over alternate methods of treating phase-equilibrium data. First, results using regression analysis are highly sensitive to the implicit or explicit weighting of the input data with no safeguard against violation of specific phase-equilibrium brackets. With MAP, the full range of solution properties consistent with a set of phase-equilibrium data can be explored without recourse to the iterative manual adjustment of input data used by Lindsley et al. (1981, p. 166) or the trial and

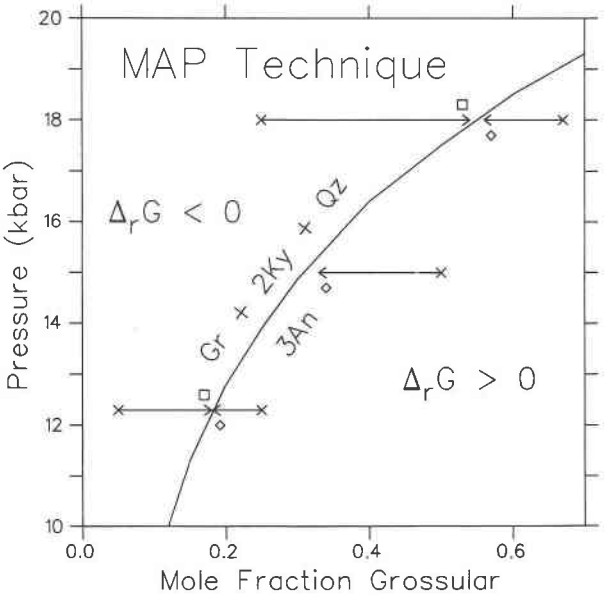

Fig. 1. Illustration of the procedure used to derive solution properties for garnet from constant temperature experiments on the displacement of the equilibrium 3An = Gr + 2Ky + Qz. Crosses and arrowheads show the starting and final garnet compositions, respectively. Uncertainties in pressure and final compositions are incorporated into the $P-X_{Gr}$ location of constraints used in the analysis. Squares and diamonds represent inequality brackets with $\Delta_r G < 0$ and $\Delta_r G > 0$; respectively.

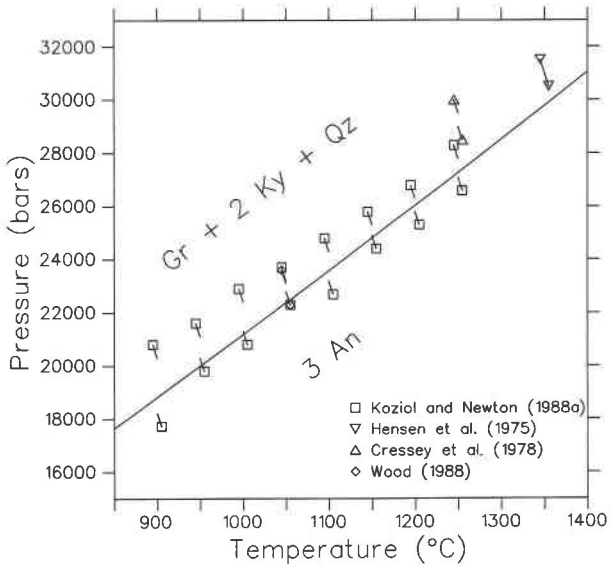

Fig. 2. Comparison of various experimental brackets for the equilibrium 3An = Gr + 2Ky + Qz with its position calculated with the thermodynamic data of Berman (1988). Open symbols represent location of experiments after adjustment of nominal values (end of lines) for estimated P-T uncertainties. The data of Koziol and Newton (1988a) and Wood (1988) have been adjusted downward by 0.2 kbar for friction effects (see text). The uncorrected data of Hensen et al. (1975) and Cressey et al. (1978) shown in this figure appear to require downward adjustment of about 1 kbar, presumably owing to friction effects.

error calibration used by Saxena and Chatterjee (1986, p. 828). Second, uncertainties in determining compositions of experimental products can be explicitly incorporated, thus allowing for realistic exploration of the constraints provided by any experimental data. Third, MAP makes use of the constraints provided by half-brackets on the position of an equilibrium without making the erroneous assumption that equilibrium has been reached. This last point is very important, as most experimental studies produce half-brackets that cannot be combined into full reversals.

Prior to the MAP analysis, excess-volume parameters were fixed by analysis of measured volumes on each of the binary joins. Excess-entropy parameters were similarly fixed for the grossular-pyrope join, the only binary for which direct excess-entropy measurements have been made. Every attempt has been made to adhere to the philosophy that the adopted solution model be only as complex as required by the experimental data and associated uncertainties.

Although inequality constraints representing 2σ uncertainties of excess enthalpies could be analyzed simultaneously with the phase-equilibrium data, this procedure has not been followed here because of the repeated occurrence of inconsistencies between phase-equilibrium data and measured heats of mixing. Instead, phase-equilibrium data have been used to form the primary constraints on enthalpies and entropies of mixing, whereas heat-of-mixing data were used to optimize the final properties with a nonlinear least-squares objective function (Berman et al., 1986). The lesser weight given to the latter data can be rationalized by the common occurrence within individual sets of enthalpy measurements of outliers that do not agree with 2σ uncertainties with either smooth analytical representations of the entire data set or with duplicate measurements (Figs. 3a, 6a, 8a). In contrast, taking account of compositional uncertainties in phase-equilibrium experiments generally suffices to correct for any overstepping of inferred equilibrium boundaries indicated by nominal compositions, although inconsistencies among data sets can arise that need to be resolved.

Calibration of binary joins

Table 2 summarizes the phase-equilibrium data that have been used to constrain thermodynamic properties. The thermodynamic activity of a mineral component is calculated from the pressure difference between the position of an equilibrium with end-member minerals and the position of the same equilibrium with the solid solution. It is therefore important to establish and correct for any differences among the positions of the end-member curves computed with the thermodynamic data used in this study and the experimentally determined end-member curves. In this study preference is given to the position of the thermodynamic end-member curves, as the thermodynamic data have been refined using an ex-

TABLE 2. Phase-equilibrium data used to derive garnet solution properties

Equilibrium	Ref.*	Uncertainties used in MAP analysis	Pressure assembly	Pressure adjustments (see text)
(A) 3An = Gr + 2Ky + Qz	1	0.3 kbar, 5° C, 0.01 X_{Gr}	¾ in. (1.905 cm) NaCl	−0.2 kbar as suggested by Koziol and Newton (1988) for ¾ in. (1.905-cm) NaCl cells
	2	0.3 kbar, 5° C, 0.01 X_{Gr}	¾ in. (1.905 cm) NaCl	−0.2 kbar as suggested by Koziol and Newton (1988) for ¾-in. (1.905-cm) NaCl cells; −0.3 kbar to account for An composition
	3	0.5 kbar, 5° C, 0.01 X_{Gr}	½ in. (1.27 cm) talc	−1 kbar as suggested by comparison of data for end-member curve (Fig. 2)
	4	0.5 kbar, 5° C, 0.01 X_{Gr}	½ in. (1.27 cm) talc	> −1 kbar as suggested by comparison of data for end-member curve (Fig. 2)
(B) An + 6Ilm + 3Qz = Gr + 2Alm + 6Rt	6	0.3 kbar, 5° C, 0.01 X_{Gr}	1 in. (2.54 cm) NaCl	−0.5 kbar to account for final compositions reported for An and Ilm
(C) 3Fa + 3An = Gr + 2Alm	5	0.3 kbar, 5° C, 0.01 X_{Gr}	1 in. (2.54 cm) NaCl	
(D) 3En + Alm = 3Fs + Py	7	0.3 kbar, 10° C, 0.01 X_{En}, X_{Alm}	NaCl and CsCl	
	8	10% kbar, 20° C, 0.01 X_{En}, X_{Alm}	Tetrahedral anvil	Only data with crystalline starting materials used
	9	1.0 kbar, 5° C, 0.01 X_{En}, X_{Alm}	Talc and Pyrex	Only data with crystalline starting materials in C capsules used
(E) Ann + Py = Phl + Alm	10	0.2 kbar, 5° C, 0.01 X_{Ann}, X_{Py}	Cold seal	

* References: (1) Koziol and Newton (1988a), (2) Wood (1988), (3) Hensen et al. (1975), (4) Cressey et al. (1978), (5) Bohlen et al. (1983a), (6) Bohlen and Liotta (1986), (7) Lee and Ganguly (1988), (8) Harley (1984), (9) Kawasaki and Matsui (1983), (10) Ferry and Spear (1978).

perimental database that extends far beyond the equilibria listed in Table 2 (see Berman, 1988, for details). In addition, this assumption leads to fulfillment of one of the goals of this work: to provide petrologists with an internally consistent set of standard-state and solution properties of minerals that can be applied meaningfully to natural assemblages.

Figure 2 shows the position of Equilibrium A computed with the thermodynamic data of Berman (1988) in comparison with brackets determined in four studies aimed at measuring grossular activity by the displaced equilibrium method. The computed curve agrees with the overall distribution of Koziol and Newton's (1988a) data, which have been adjusted downward in pressure by 0.2 kbar to account for their estimation of friction effects in ¾-in. (1.905-cm) NaCl pressure assemblies, although the curve is displaced to the low-pressure uncertainty limit (0.54 kbar estimated by Koziol and Newton) of the 950 and 1050 °C brackets. These small differences may be indicative of slightly greater friction effects than they estimate or by upward displacement of the equilibrium caused by incorporation of small amounts of Li (from the Li_2MoO_4 flux) into the feldspar structure. In either case this small difference can be ignored in analyzing their displaced phase equilibrium data, as the friction effects should be smaller at the lower pressures of the displaced equilibrium experiments, and contamination by Li should affect both the displaced and the end-member data equally.

At 1050 °C, Wood (1988) reversed Equilibrium A between 23.0 and 23.5 kbar using a piston cylinder apparatus with a ¾-in. (1.905-cm) NaCl pressure assembly. As these brackets are virtually identical to those found by Koziol and Newton (1988a), Wood's data have also been adjusted downward by the 0.2-kbar friction correction recommended by Koziol and Newton for ¾-in. NaCl pressure assemblies. Comparison of the 1300 and 1350 °C brackets of Hensen et al. (1975) and Cressey et al. (1978) with the computed equilibrium curve (Fig. 1) indicates a 1-kbar correction toward lower pressure. This correction represents a minimum value that should be applied to their displaced equilibrium data collected at lower temperatures where friction effects would be expected to increase.

Grossular-Almandine

Reversed experimental data relevant to analysis of the Gr-Alm join have been obtained by Koziol and Newton (1988b) for Equilibrium A and by Bohlen and Liotta (1986) and Bohlen et al. (1983b), respectively, for equilibria involving garnet of the composition $Gr_{1/3}Alm_{2/3}$:

$$An + 6\ Ilm + 3\ Qz = Gr + 2\ Alm + 6\ Ru \quad (B)$$

and

$$3\ Fa + 3\ An = Gr + 2\ Alm. \quad (C)$$

Retrieval of mixing properties from these data is critically dependent on assumed standard-state thermodynamic data. In order to reproduce all phase-equilibrium data as closely as possible on this join, minor adjustments were made to the standard state properties of almandine and ilmenite given by Berman (1988) and derived without consideration of mixing properties on this join. These revised standard state properties (Table 3) are consistent with all other thermodynamic properties given by Berman (1988) and with the same phase equilibrium experiments used by Berman (1988) to derive these properties. It is encouraging that these revisions lead to very close

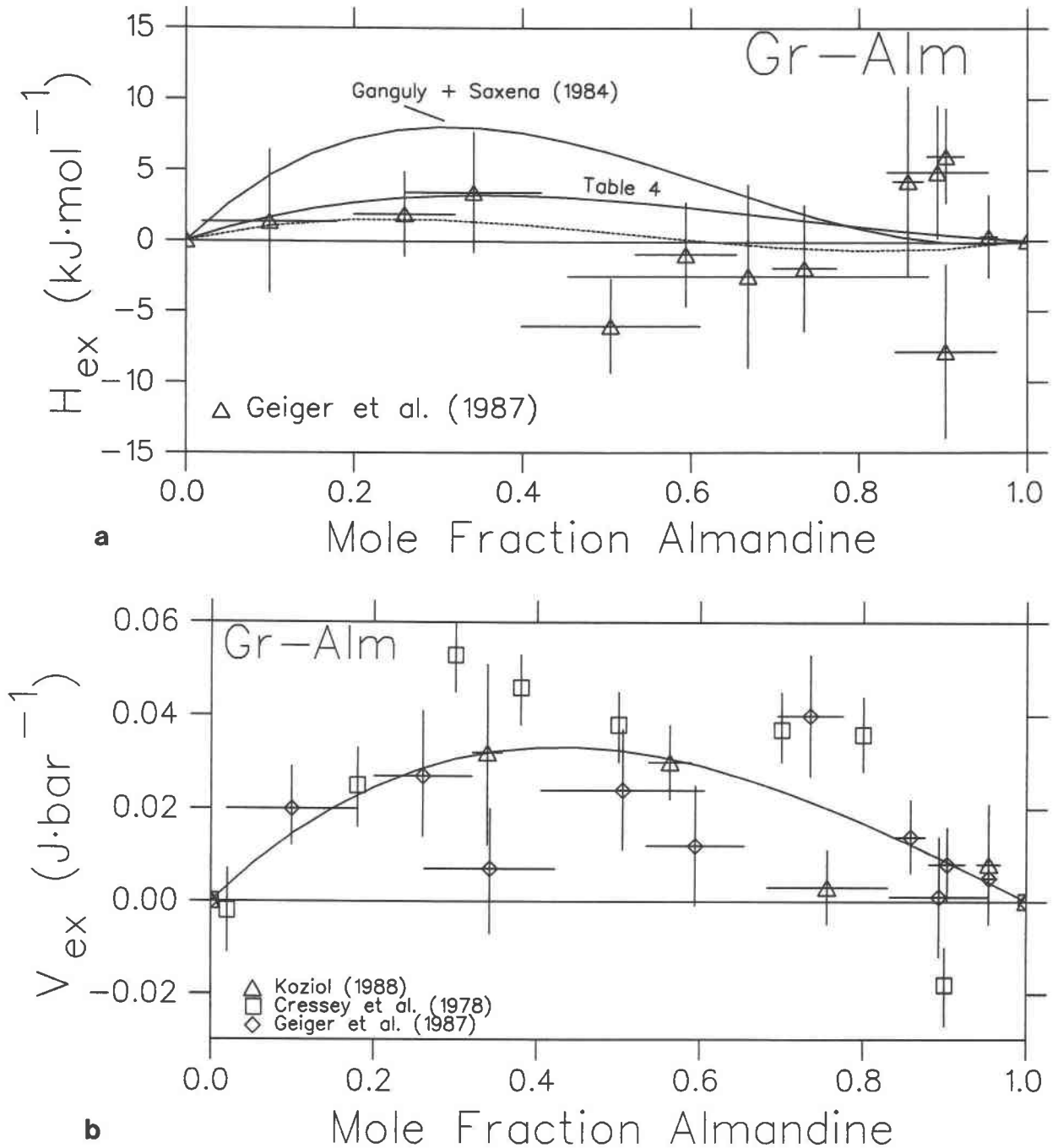

Fig. 3. Comparison of predicted and measured values for (a) heats of mixing and (b) volumes of mixing on the grossular-almandine join. Error bars show 2σ uncertainties that incorporate uncertainties in end-member values. Predicted curves are also shown in (a) for models of Geiger et al. (1987; dashed curve) and Ganguly and Saxena (1984). Note in (b) that the suggestion of negative excess volume (Cressey et al., 1978) for almandine-rich compositions is not supported by more recent data.

agreement of the enthalpy of the formation of almandine (−5267.216 kJ/mol) with that (−5267.8 kJ/mol) derived from electrochemical measurements reported recently by Woodland and Wood (1989).

Although the data for Equilibria A and B are compatible with near-ideal mixing with no excess entropy, the highest temperature bracket for Equilibrium C requires a minimum symmetric entropy of about 9 J/(mol K). However, this amount of excess entropy leads to excess heats of mixing that are considerably larger than measured by

TABLE 3. Standard-state thermodynamic properties of minerals (at 1 bar and 298.15 K) modified from Berman (1988)

Mineral	Formula	$\Delta_f H$ (kJ/mol)	S° [J/(mol K)]	V (J/bar)
Almandine	$Fe_3Al_2Si_3O_{12}$	−5267.216*	340.007*	11.511†
Annite	$KFe_3AlSi_3O_{10}(OH)_2$	−5142.800‡	420.000‡	15.408‡
Ilmenite	$FeTiO_3$	−1232.448*	108.628†	3.17†
Phlogopite	$KMg_3AlSi_3O_{10}(OH)_2$	−6210.391§	334.346§	14.977†

Note: Heat-capacity and volume functions are given by Berman (1988) for all minerals except annite: $C_P = 727.21 - 4775.04T^{-1/2} - 13\,831\,900\,T^{-2} + 2\,119\,060\,000\,T^{-3}$ (C_P in J/(mol K); estimation based on exchange reaction to phlogopite) $V_{(P,T)}/V_{(1\ bar,\ 298.15\ K)} = 1 + (3.445 \times 10^{-5})(T - 298.15) - (1.697 \times 10^{-6})(P - 1)$ (same as phlogopite).

* Properties revised on the basis of experimental data involving garnet solid solutions discussed in this paper.

† Properties taken from Berman (1988).

‡ Properties derived from garnet-biotite data of Ferry and Spear (1978) in conjunction with garnet properties given in Table 4 and the assumption of ideal Fe-Mg mixing in biotite.

§ Properties revised to account for data of Wood (1976) and Peterson and Newton (1988) for the equilibrium phlogopite + quartz = enstatite + sanidine + H_2O.

Geiger et al. (1987). A small adjustment (0.3 kbar) beyond the uncertainty reported by Bohlen et al. (1983b) for this bracket permits a smaller excess entropy (5.08 J/(mol K) and heats of mixing that are in good agreement with the data of Geiger et al. (Fig. 3a). The amount of this adjustment is within the uncertainties of the thermodynamic properties of minerals in Equilibrium C and may indicate that minor revisions in some heat capacity and volume functions are necessary. The adopted solution properties (Table 4) are consistent with both sets of phase-equilibrium data for the $Alm_{2/3}Gr_{1/3}$ composition (Fig. 4) and with Koziol and Newton's (1988b) data (Fig. 5). The data of Cressey et al. (1978) were not used because they are clearly inconsistent with those of Koziol and Newton (Fig. 5) since similar garnet compositions were produced about 3 kbar higher in the experiments of Cressey et al. The simplest interpretation is that this discrepancy results from much larger friction effects in the experiments of Cressey et al. at 1000 °C than the 1-kbar correction implied by comparison of their 1350-°C reversal of the end-member equilibrium with the computed position and with the other data sets (Fig. 2).

Excess volumes measured by Geiger et al. (1987) and Koziol (1988) are positive across the entire grossular-almandine join, contradicting the suggestion of negative excess volume for almandine-rich compositions (Cressey et al., 1978; see Fig. 3b). The present two parameter representation of the volume data is asymmetric toward grossular-rich compositions, the same shape exhibited in heats of mixing derived from the above analysis (Fig. 3a). This parallelism can be viewed most simply as the energetic response to the observed volume mismatch.

The model yields enthalpies of mixing that are less strongly nonideal than the models of Ganguly and Saxena (1984) and Anovitz and Essene (1987). This difference can be attributed to the previous workers' use of (a) phase equilibrium data of Cressey et al. (1978), which are sys-

TABLE 4. Garnet solution properties (only nonzero values) to be used with Equations 1 and A1–A4

Parameter	W_H (J/mol)	W_S [J/(mol K)]	W_V (J/bar)
112	21 560	18.79	0.10
122	69 200	18.79	0.10
113	20 320	5.08	0.17
133	2620	5.08	0.09
223	230		0.01
233	3720		0.06
123	58 825	23.87	0.265
124	45 424	18.79	0.100
134	11 470	5.08	0.130
234	1975		0.035

Note: Component order: 1 = Gr, 2 = Py, 3 = Alm, 4 = Sp. Ternary terms were calculated from binary parameters with Equation 2; ternary parameters of Wohl equation, C_{ijk}, are all equal to zero.

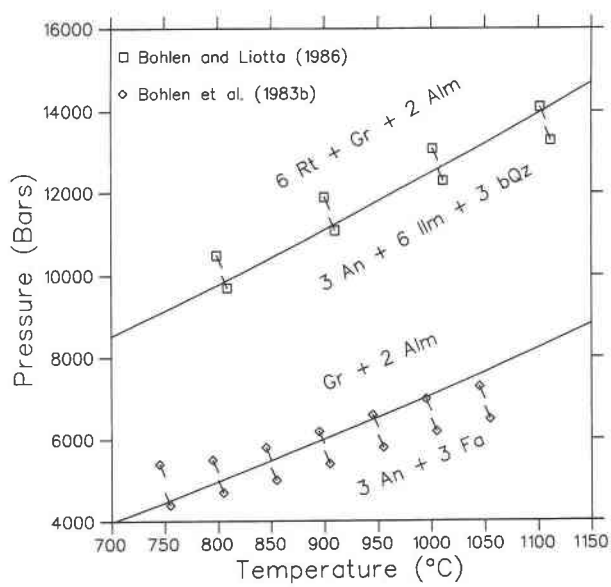

Fig. 4. Comparison of experimental data for two equilibria involving $Gr_{1/3}Alm_{2/3}$ garnets with positions computed with thermodynamic data from Tables 3 and 4. Symbols as in Fig. 2. The brackets for the high pressure equilibrium have been adjusted down by 0.5 kbar, the displacement calculated (assuming ideal mixing) for the reported compositions of anorthite and ilmenite (Table 2). See text for discussion of the inconsistency with the high temperature bracket for the Gr + 2Alm = 3An + 3Fa equilibrium.

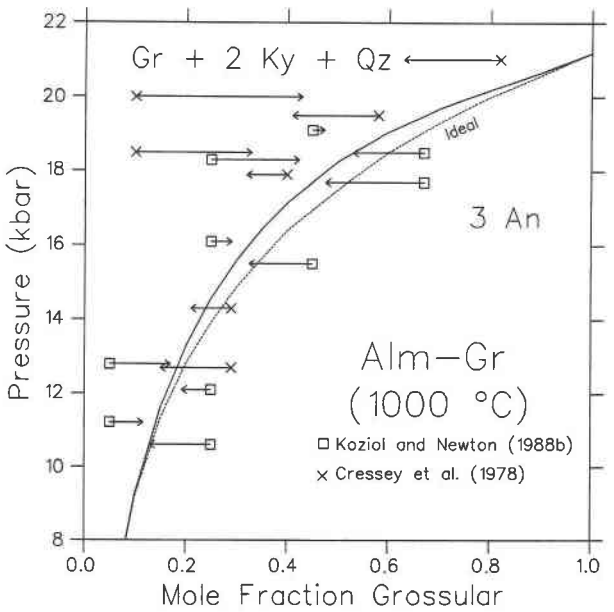

Fig. 5. Comparison of experimental brackets for the displacement of the equilibrium 3An = Gr + 2Ky + Qz in the almandine-grossular system with its position calculated assuming ideal mixing (dashed curve) and with the thermodynamic data given in Tables 3 and 4 (solid curve). Symbols with arrows show starting and final garnet compositions, respectively. The final compositions and pressures have been adjusted for uncertainties (Table 2). Note the displacement to higher pressure of the results of Cressey et al. (1978) that suggests the need for a large friction correction.

tematically higher in pressure than those of Koziol and Newton (see above), (b) Haselton and Newton's (1980) model for grossular-almandine excess volume that incorporates negative departures from ideality for almandine-rich compositions, and (c) a larger excess-entropy parameter for the grossular-almandine join [18.828 J/(mol K) in the model of Ganguly and Saxena (1984) and in Anovitz and Essene's (1987) model I; 34.2 J/(mol K) in Anovitz and Essene's model II]. In comparison to the analysis of Anovitz and Essene (1987), the smaller excess entropy derived in this study largely reflects the effect of adopting standard-state properties here that are in better agreement with the results of Bohlen et al. (1983a), which showed high-temperature reversals for the equilibrium

$$\text{Alm} + 3\ \text{Ru} = 3\ \text{Ilm} + \text{Si} + 2\ \text{Qz}$$

[compare Fig. 1 of Anovitz and Essene (1987) with Fig. 44b of Berman (1988)]. Nevertheless, because of the extreme sensitivity of excess entropy to small perturbations of both phase-equilibrium and thermodynamic data, additional experiments that span a wider range of temperature are required to fix this value more confidently.

Grossular-Pyrope

Excess volumes on the grossular-pyrope join are poorly constrained by the data (Fig. 6b). Within the context of the amount of scatter within and the degree of correspondence among various data sets, it is difficult to justify a more complicated representation than the symmetric model adopted in this study. This model contrasts with those that incorporate negative departures from ideality (e.g., Haselton and Newton, 1980; Ganguly and Saxena, 1984) and near ideal mixing (Wood, 1988) near the pyrope end-member.

An excess entropy of 4.51 J/(mol K) was measured by Haselton and Westrum (1980) on a synthetic garnet of composition $X_{Gr} = 0.4$. Following Haselton and Newton (1980), and consistent with the above representation of the volume data, the simplest assumption is that the entropy is a symmetric function, giving $W_s = 18.79$ J/(mol K). In contrast, Wood (1988) argues that W_s has the same dependence on composition as W_V, is thus strongly asymmetric, and is nearly zero near the pyrope end-member.

Wood's reversals of garnet compositions $X_{Gr} = 0.128$ and 0.150 at 15 and 16 kbar agree with the half-brackets of Hensen et al. (1975), but the combined data (Fig. 7) for garnet compositions with $X_{Gr} < 0.22$ do not place very stringent constraints on mixing properties across this join. With the above approximations for excess entropy and volume, the enthalpy of mixing can be described as nearly symmetric to highly asymmetric toward pyrope-rich compositions. The latter alternative has been adopted in this study because it produces heats of mixing compatible with the measurements of Newton et al. (1977; Fig. 6a). It should be noted however that a symmetric fit (e.g., $W_{12} = 41.4$ kJ/mol given by Hodges and Spear, 1982) also represents these data reasonably well, but this alternative would require a considerably smaller excess entropy than derived by Haselton and Westrum (1980) in order to reproduce the phase-equilibrium data. Further experimental work involving more grossular-rich garnet and analysis of well-defined natural assemblages are needed to reduce this remaining uncertainty.

Pyrope-Almandine

Recent volume measurements (Geiger et al., 1987) indicate near-ideal mixing for the pyrope-almandine binary, consistent with the similarity in ionic radii of Fe^{2+} and Mg^{2+}. The best representation of these data suggests small positive deviations from ideality with asymmetry towards the Fe end-member (Fig. 8b). The same sense of asymmetry but with much larger magnitude is observed in the heat-of-mixing data of Geiger et al. (1987; Fig. 8a) and was deduced by Ganguly and Saxena (1984) from an analysis of Mg-Fe fractionation among natural mineral pairs.

A great deal of experimentally determined Mg-Fe exchange data between garnet and other minerals can be used to derive garnet mixing properties on this join, but conclusions are highly dependent on the assumed properties of the other minerals involved in the experiments. It seems clear that the best strategy is to process all data together so as to extract simultaneously a consistent set

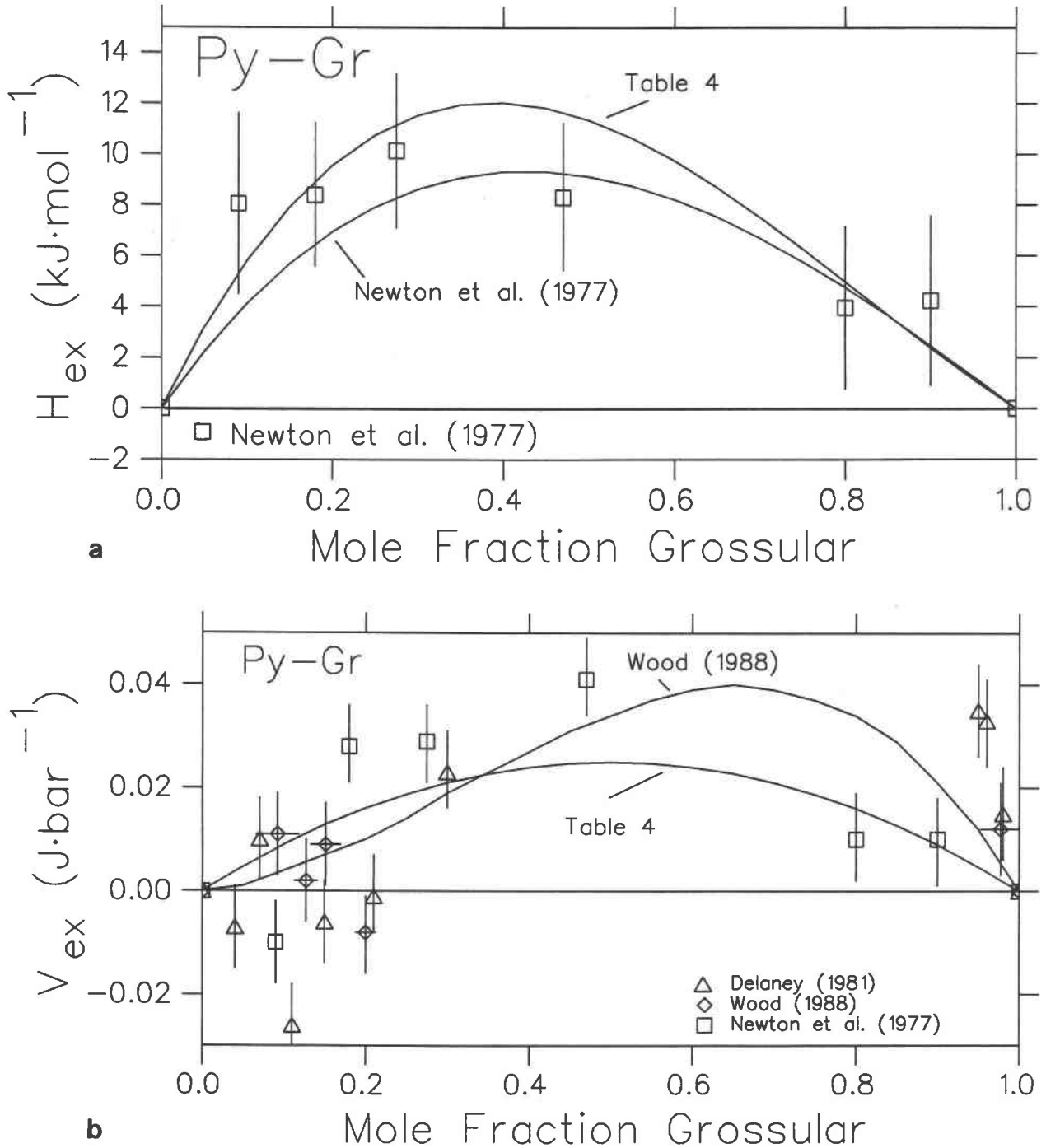

Fig. 6. Comparison of predicted and measured values for (**a**) heats of mixing and (**b**) volumes of mixing on the join pyrope-grossular. Error bars show 2σ uncertainties that incorporate uncertainties in end-member values. Note the large discrepancies among various volume determinations (b) near both end-members.

of solution properties for all minerals (Engi et al., 1984). This is the only procedure that can effectively reduce the possibility of erroneous assumptions regarding the solution properties of any one mineral misleading the interpretation of the properties of another mineral, in this case garnet. Although the wisdom of this approach seems indisputable, the magnitude of this task is considerable and beyond the scope of this study. Instead the procedure adopted here is to derive garnet properties from consideration of experimental exchange data between orthopy-

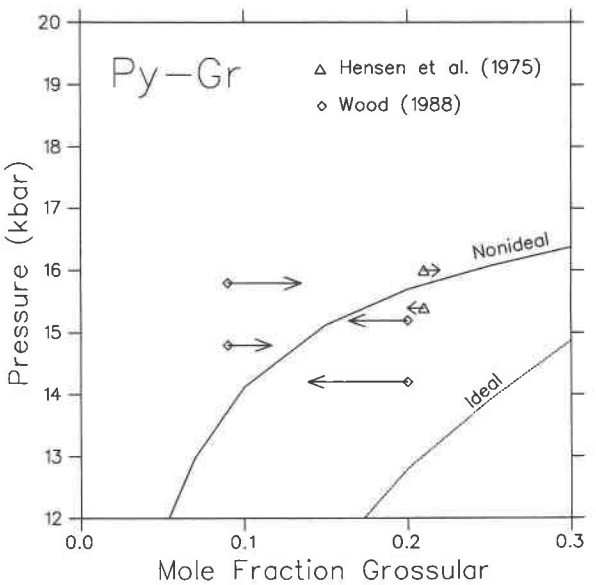

Fig. 7. Comparison of experimental brackets for the displacement of the equilibrium 3An = Gr + 2Ky + Qz in the pyrope-grossular system with its position calculated assuming ideal mixing (dashed curve) and with the thermodynamic data given in Tables 3 and 4 (solid curve). Symbols as in Fig. 5. The data of Wood have been corrected to lower pressure to account for the reduced activity of anorthite in his experiments. The data of Hensen et al. (1975) have been corrected to account for the presence of kyanite instead of sillimanite and adjusted downward by 1 kbar as suggested by comparison of their bracket with the data of Koziol and Newton (1988a) for the end-member curve (Fig. 2).

roxene and garnet, and then to form an independent test of the derived properties by applying them to natural assemblages that do not contain orthopyroxene.

The assumption adopted in this study is that orthopyroxene can be well approximated at high temperature as a two-site ideal solution. Many activity measurements for Mg-Fe orthopyroxenes suggest near-ideal mixing (e.g., Kitayama and Katsura, 1968; Sakawa et al., 1978). In contrast, recent data of Sharma et al. (1987) gathered at lower temperature (727 °C) indicate positive excess heats of mixing, but these can be expected to more closely approach ideality at higher temperatures. Many workers have also concluded that the two-site ideal mixing model provides the most reasonable thermobarometric results for a wide range of natural assemblages (e.g., Wood and Banno, 1973; Newton, 1983; Perkins and Chipera, 1985). Such a model is admittedly oversimplified in that it ignores the effects of cation ordering for which there are conflicting descriptions (Davidson and Lindsley, 1989; Sack and Ghiorso, 1989). These effects are most important, however, at temperatures lower than those of the most constraining experiments used in the following analysis. An additional complication is introduced by possible nonideal interactions related to Al solubility in orthopyroxene. This should have a negligible effect in the analysis because the most constraining experimental data discussed below involve pyroxenes with less than 2.75 wt% Al_2O_3.

Table 2 summarizes the three sets of experiments on the equilibrium

$$3\ \mathrm{En} + \mathrm{Alm} = 3\ \mathrm{Fs} + \mathrm{Py}. \qquad (D)$$

The data of Lee and Ganguly (1988) constitute the most extensive set of data with K_D values reversed from both directions. Kawasaki and Matsui (1983) provide much data at 1100 and 1300 °C, but the present analysis utilizes only those data in which the direction of change in K_D values was reported and which were produced with crystalline starting materials. The data of Harley (1984) are difficult to use with confidence because many of the experiments were conducted in Fe capsules and orthopyroxene-garnet charges suffered differential iron addition. Comparison of the compositions of phases contained in Fe and C capsules along with textural criteria were used by Harley to estimate corrections in Fe-Mg ratios of the Fe capsule run products. Rather than base any conclusions on Harley's interpretations on the effects of Fe addition and zoning profiles, I used only Harley's experiments with C capsules in this analysis.

Using the standard-state properties given by Berman (1988) with or without the almandine revision of this study (see grossular-almandine section above), the combined data are nearly consistent with ideal mixing in orthopyroxene and garnet (Figs. 9a, 9b). Only small discrepancies occur with the highest temperature data of all three studies. In order to reproduce all valid experimental half-brackets, it is necessary to allow for small positive excess heats of mixing in garnet that show the same sense of asymmetry as measured volumes and heats of mixing (Fig. 8) but which are much smaller in magnitude than those suggested by the calorimetric data. A closer representation of the excess enthalpies could be obtained by allowing for positive excess entropy, but the very small observed volumes of mixing are more consistent with smaller excess heats retrieved here. In fact, the average of the derived mixing parameters is in reasonable accord with a symmetrical excess enthalpy of 1.32 kJ/mol predicted with the empirical model of Davies and Navrotsky (1983) that is based on the correlation of volume mismatch with excess enthalpy. It should be noted that the exact values of the excess parameters derived here for the pyrope-almandine join are dependent on the computed Ca-Fe mixing properties because the latter influence the derived thermodynamic properties of almandine.

Ganguly and Saxena (1984) derived Fe-Mg mixing parameters based on a regression analysis of K_D values of natural assemblages; standard-state mineral properties used in their study were not reported. Their predicted mixing parameters (Fig. 8a) agree with the data of Geiger et al., but lead to large discrepancies with the orthopyroxene-garnet data at low X_{Fe} (Fig. 9a). Because of the possibility of introducing a systematic error in garnet

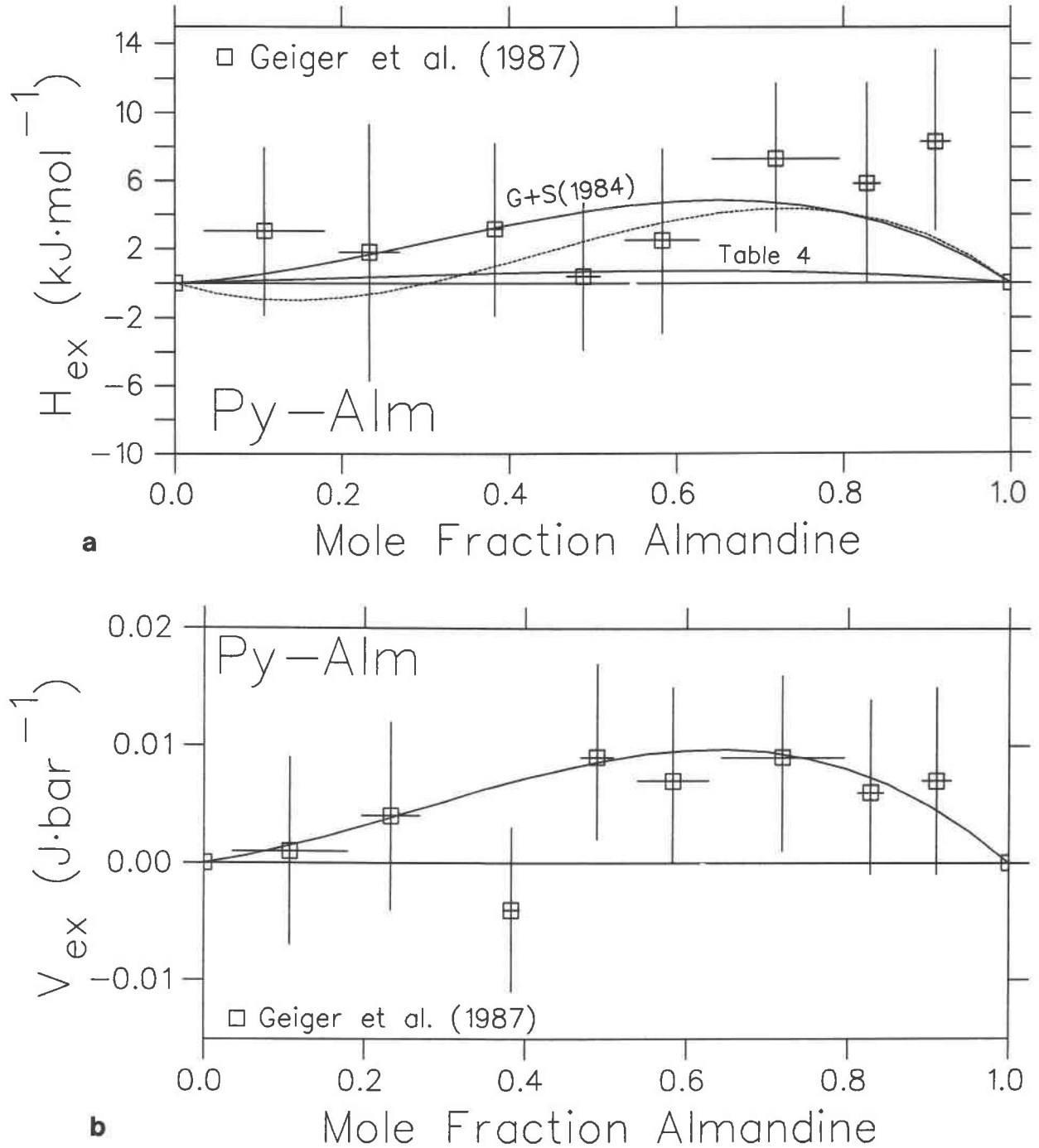

Fig. 8. Comparison of predicted and measured heats (a) and volumes (b) of mixing on the join pyrope-almandine. Error bars show 2σ uncertainties that incorporate uncertainties in end-member values. In (a) heat of mixing curves are also shown for the models of Ganguly and Saxena (1984) and Geiger et al. (1987; dashed curve).

properties as a result of the assumption of ideal mixing in orthopyroxene, it is desirable to form an independent check on the Fe-Mg mixing properties derived above. One effective method described below involves the use of phase equilibrium data to extract thermodynamic data that depend on garnet Fe-Mg mixing properties and then to test these new thermodynamic data against information gleaned from natural assemblages.

The Fe-Mg exchange data of Ferry and Spear (1978) for the garnet-biotite equilibrium,

$$\text{Ann} + \text{Py} = \text{Phl} + \text{Alm} \qquad \text{(E)}$$

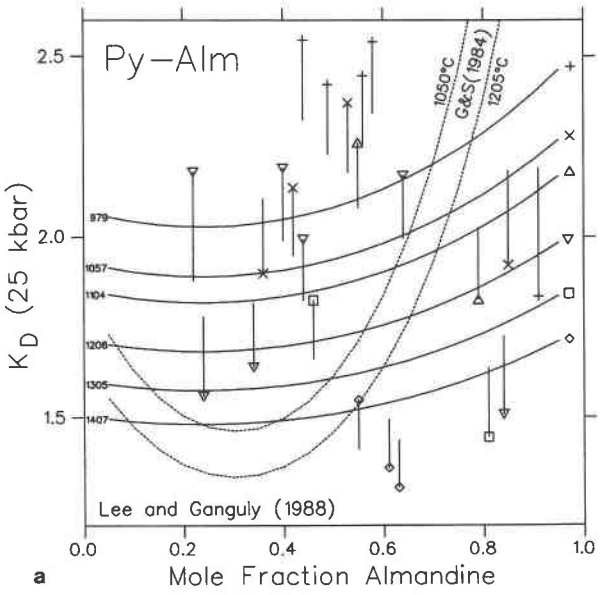

Fig. 9a. Comparison of Lee and Ganguly's (1988) K_D brackets for the equilibrium 3Fs + Py = 3En + Alm in the pyrope-almandine system with its position calculated with the thermodynamic data given in Tables 3 and 4 (solid curves). All experimental data have been corrected to 25 kbar using the volume data given in Tables 3 and 4 and by Berman (1988). Calculated curves and symbols marked on the right correspond to various experimental temperatures. Symbols show the extremes of experimental K_D data calculated with 0.01 uncertainties in the mole fractions of analyzed garnet and pyroxene compositions. Connecting lines show experimental K_D values, unadjusted for compositional uncertainties and point in the direction in which equilibrium was approached during the course of each experiment. Note the large inconsistencies between the data and predicted K_D's at 1050 and 1205 °C using the model of Ganguly and Saxena (1984; dashed curves) extrapolated to lower X_{Alm} than their recommended limit ($X_{Alm} = 0.75$).

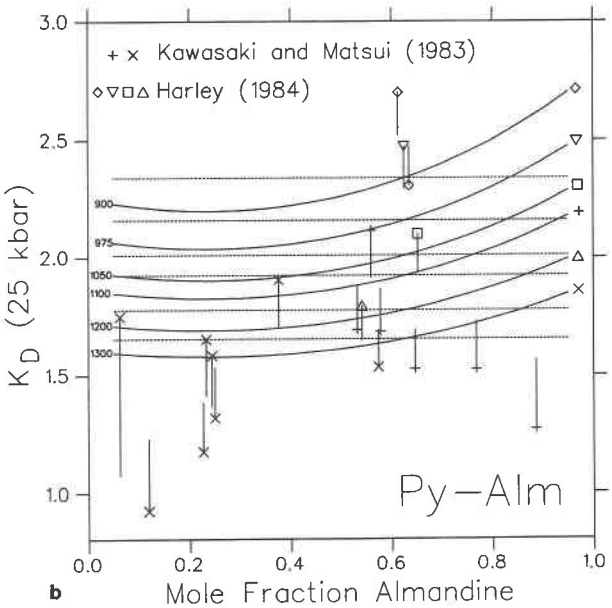

Fig. 9b. Comparison of K_D brackets for the equilibrium 3Fs + Py = 3En + Alm in the pyrope-almandine system with its position calculated assuming ideal mixing (dashed curves) and with the thermodynamic data given in Tables 3 and 4 (solid curves). All experimental data have been adjusted to 25 kbar using the volume data given in Tables 3 and 4 and by Berman (1988). Symbols as in Fig. 9a.

have been used to derive the standard-state enthalpy of formation for annite with standard-state properties for the other minerals in Equilibrium E given by Berman (1988) and in Table 3. Ideal Fe-Mg mixing in biotite is assumed following Mueller's (1972) analysis of natural K_D data and the experimental data of Wones and Eugster (1965). This assumption is also consistent with unit-cell refinements of Hewitt and Wones (1975), which show no deviation from a linear correlation between volume and composition on the annite-phlogopite join. Because the annite properties depend on garnet Fe-Mg mixing, two alternative values have been extracted, one using the properties derived in this study (Table 4, −5142.8 kJ/mol) and the other (−5160.0 kJ/mol) using the Fe-Mg garnet mixing properties of Ganguly and Saxena (1984). The large difference between the values derived for annite is a direct consequence of the differences in activity coefficients calculated for pyrope and almandine with the two models noted above. Comparison of how closely the two sets of annite-bearing equilibria correspond to other equilibria in applications to natural assemblages then forms an independent test of the proposed Fe-Mg mixing properties.

For the purpose of this test, analytical data have been used from muscovite-bearing pelites that straddle the kyanite-sillimanite isograd at Azure Lake, British Columbia (Pigage, 1982), and other muscovite-bearing assemblages interpreted to have equilibrated near the Al-silicate triple point at Mount Moosilauke, New Hampshire (Hodges and Spear, 1982). Compositional homogeneity of minerals on a thin-section scale and systematic element partitioning between minerals suggest that equilibrium was closely approached. In order to test the two sets of annite properties, comparison is made between pressures computed from Equilibrium A and the equilibrium

$$\text{Ann} + 2\ \text{Al}_2\text{SiO}_5 + \text{Qz} = \text{Ms} + \text{Alm}. \qquad \text{(F)}$$

Activities of anorthite, muscovite, and biotite are computed from

$$a_{An} = \gamma_{An} X_{An}(1 + X_{An})^2/4$$
$$a_{Ms} = \gamma_{Ms} X_K X_{Al}^2 X_{OH}^2,$$
$$X_{Al} = {}^{[6]}\text{Al}/(\text{Fe} + \text{Mg} + \text{Mn} + \text{Ti} + {}^{[6]}\text{Al})$$
$$a_{Ann} = \gamma_{Ann} X_K X_{Fe}^3 X_{OH}^2,$$
$$X_{Fe} = \text{Fe}/(\text{Fe} + \text{Mg} + \text{Mn} + \text{Ti} + {}^{[6]}\text{Al})$$

with γ_{An}, γ_{Ms}, and γ_{Ann} computed with the models of

Fuhrman and Lindsley (1988), Chatterjee and Froese (1975), and Indares and Martingole (1985; model B), respectively. The latter model accounts for the nonideal effects of Ti and [6]Al, discussed at greater length below.

Use of the preferred thermodynamic properties of annite along with those of garnet in Table 4 yields garnet-biotite temperatures between 555 and 615 °C for the Azure Lake pelites and between 485 and 535 °C for the Mount Moosilauke pelites. Use of the second annite value along with Ganguly and Saxena (1984) garnet properties gives similar ranges of temperatures, shifted about 50 °C higher owing largely to the effects of Mn. The general similarity of results with both models reflects the fact that both sets of calculations are internally consistent and have been calibrated against the garnet-biotite experiments of Ferry and Spear (1978).

Figure 10 shows pressures computed with the preferred thermodynamic properties. For the Azure Lake pelites, Equilibrium F gives pressures that average 1 kbar higher than Equilibrium A, although for three samples excellent agreement is achieved. For the Mount Moosilauke pelites, four samples give nearly coincident pressures, and two samples give pressures about 1.5 kbar higher with Equilibrium F. In marked contrast, use of the annite properties derived with Ganguly and Saxena's (1984) garnet model yields pressures for sillimanite-bearing samples that average about 12 kbar higher with Equilibrium F than with Equilibrium A. For Azure Lake kyanite-bearing samples, the discrepancies increase to about 22 kbar. These extreme differences in the results of the two sets of calculations are a direct consequence of the assumed Fe-Mg garnet mixing properties, which are transferred to annite properties through thermodynamic analysis of experimental data for the garnet-biotite equilibrium. The magnitude of these differences reflects the low entropy of Equilibrium F, particularly with kyanite, making it an extremely sensitive test of thermodynamic input data. The reasonable pressures computed with Equilibrium F offer strong support, completely independent of the assumed orthopyroxene properties, for the Fe-Mg mixing properties derived herein as compared to those of Ganguly and Saxena (1984). The same conclusion also applies to the highly asymmetric model of Geiger et al. (1987) because of its similarity to the model of Ganguly and Saxena.

Although the above comparison supports the garnet properties derived here, the small discrepancies apparent in Figure 10 between pressures computed with Equilibria A and F warrant further attention. One complication, albeit a second-order effect, is that the Indares and Martingole (1985) model does not specify the separate interactions of Ti and [6]Al with Fe and Mg in biotite, only the $W_{MgTi} - W_{FeTi}$ and $W_{Mg[6]Al} - W_{Fe[6]Al}$ differences. The results shown in Figure 10 were computed assuming that all Ti and [6]Al interactions with Fe are zero. When interactions with Fe are assumed to be positive, pressures computed with Equilibrium F may be lowered by up to about 1 kbar, improving results for most of the Azure Lake samples but worsening them for most of the Mount Moosilauke samples. Until further work addresses the separate interactions of Ti and [6]Al with Fe and Mg in biotite, it will remain unclear whether the discrepancies shown in Figure 10 are related to these effects, to calibration of garnet mixing properties, or to subtle effects of disequilibrium in the natural samples.

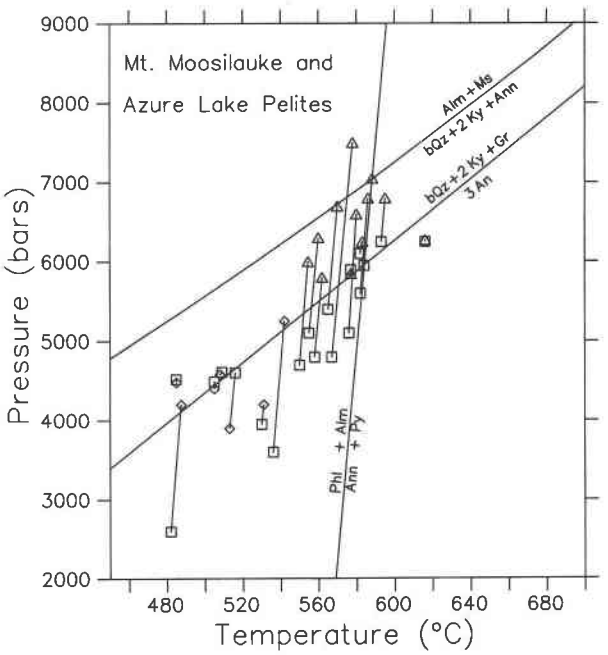

Fig. 10. Comparison of pressures derived from Equilibria A and F for muscovite-bearing pelites from Azure Lake, British Columbia (Pigage, 1982), and Mount Moosilauke, New Hampshire (Hodges and Spear, 1982), using the thermodynamic data of Tables 3 and 4 and from Berman (1988) along with other activity models discussed in the text. Temperatures are computed from the garnet-biotite equilibrium (Equilibrium E). Squares show the P-T intersections of Equilibria A and E. Intersections between Equilibria F and E are shown by triangles for the Azure Lake samples and by diamonds for the Mount Moosilauke samples.

Binary systems containing Mn

Following Ganguly and Kennedy (1974), ideal interactions are assumed on the almandine-spessartine binary, consistent with the very small difference in ionic radii of Fe^{2+} and Mn^{2+}. Recent displaced phase-equilibrium data by Koziol and Newton (1987) and Wood (1988) for Equilibrium A demonstrate that the grossular-spessartine join is ideal within uncertainties (Fig. 11). Ganguly and Kennedy (1974) and Ganguly and Saxena (1984) derived a large positive excess enthalpy of mixing on the pyrope-spessartine binary (37656 J/mol) from their analyses of Mg-Fe fractionation between garnet and coexisting phases. On the other hand, Hodges and Spear (1982) concluded that W_{MgMn} must be close to zero in order to yield garnet-biotite temperatures close to the Al-silicate triple point for Mount Moosilauke pelites. The present for-

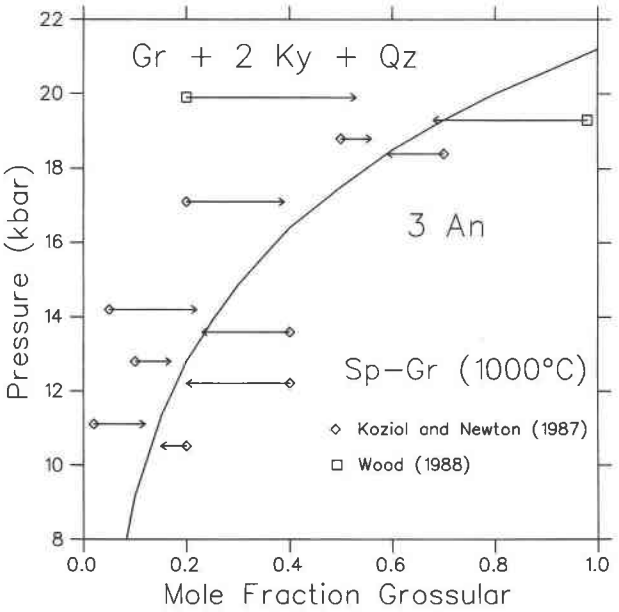

Fig. 11. Comparison of experimental brackets for the equilibrium 3An = Gr + 2Ky + Qz in the spessartine-grossular system with its position calculated assuming ideal mixing. Symbols with arrows show starting and final garnet compositions, respectively.

mulation of the garnet-biotite geothermometer using the annite properties derived above also gives the most reasonable temperatures with ideal Mg-Mn mixing. For the seven Mount Moosilauke samples ($0.09 < X_{Sp} < 0.171$), calculated temperatures at the Al-silicate triple point pressure (3.85 kbar) range from 485 to 535 °C, in agreement with the triple-point temperature of 505 °C. In contrast, use of $W_{MgMn} = 37656$ J/mol produces temperatures from 540 to 595 °C. Analysis of more Mn-rich pelites ($0.08 < X_{Sp} < 0.532$) described by Raeside et al. (1988) with $W_{MgMn} = 0$ also yields very reasonable garnet-rim biotite temperatures for assemblages with chlorite-albite (390 °C), chlorite-plagioclase (425–455 °C), biotite (446–510 °C), and sillimanite (485–610 °C). For the same assemblages, use of $W_{MgMn} = 37656$ J/mol yields 613 °C, 621–654 °C, 580–645 °C, and 660–790 °C. The latter set of temperatures is unrealistically high for the lower-grade rocks and does not show the same consistent correlation with increasing metamorphic grade.

Calibration of ternary interactions

With the exception of the recent study by Koziol and Newton (1988b, 1988c) on Ca-Mg-Fe garnets, experimental data that can be used to constrain ternary garnet interactions are almost entirely lacking. MAP analysis of the preliminary experiments reported by Koziol and Newton (1988b) on displacement of Equilibrium A with Ca-Mg-Fe garnet solutions suggests that these data are compatible with a Wohl ternary C_{123} interaction parameter equal to zero, assuming the binary mixing properties given in Table 4. Accordingly, and in marked contrast to the model of Ganguly and Saxena (1984), the ternary Wohl parameters have been set to zero for this and the other three ternaries in the quaternary garnet system.

Discussion

One of the ultimate goals of theoretical petrology is to provide thermodynamic data that allow one to calculate the same unique pressure and temperature from any of the equilibria implied by a mineral assemblage that equilibrated at the same P and T and for which accurate compositional data are available (Powell and Holland, 1988; Berman and Brown, 1988). In order to achieve this goal, accurate solution models are needed, as well as accurate standard-state properties. A great deal of attention has been focused recently on providing refinements in both types of thermodynamic data in order to obtain compatibility of different geobarometers in various chemical systems (e.g., Newton and Perkins, 1982; Anovitz and Essene, 1987; Moecher et al., 1988). Although not independent of standard-state thermodynamic data, multi-equilibrium P-T calculations provide one of the most stringent tests for solution models because, barring a fortuitous cancellation of errors, convergence in a single P-T region can only be achieved if all calculated component activity coefficients are close to correct. A number of granulites have been studied, and Figure 12 shows typical graphical results of P-T calculations for a two-pyroxene granulite studied by Coolen (1980). Using the activity models of Fuhrman and Lindsley (1988) for anorthite, Newton (1983) for clinopyroxene and orthopyroxene, and this paper for garnet, together with standard-state data of Table 3 and from Berman (1988), P-T intersections of metastable and stable equilibria are produced within a very narrow P-T window, spanning 20 °C and 0.4 kbar (small dotted region in Fig. 12). In contrast, use of the Moecher et al. (1988) or Ganguly and Saxena (1984) mixing properties for garnet leads to much wider divergence among these intersections, ranging over 200 °C and 5.0 kbar. This example highlights some of the major differences that can be produced using different solution models, a point that is further emphasized by the fact that pressures computed with individual barometers shown in Figure 12 are up to 3 kbar higher using the garnet models of Moecher et al. (1988) and Ganguly and Saxena (1984).

A significant problem in testing solution models is that convergence in P-T values derived from various equilibria is only one of the conditions necessary to be satisfied—some means of assessing the accuracy of the convergence zone must be devised. In addition, all mineral compositions may not have quenched at the same pressure and temperature. Newton and Haselton (1981) and later Ganguly and Saxena (1984) tested Al-silicate-bearing rocks by comparing pressures computed with Equilibrium A with the Al-silicate phase diagram. In order that results can be compared directly with these other two models, the same test is applied here. Although this test suffers from the limitations discussed above, a minimum

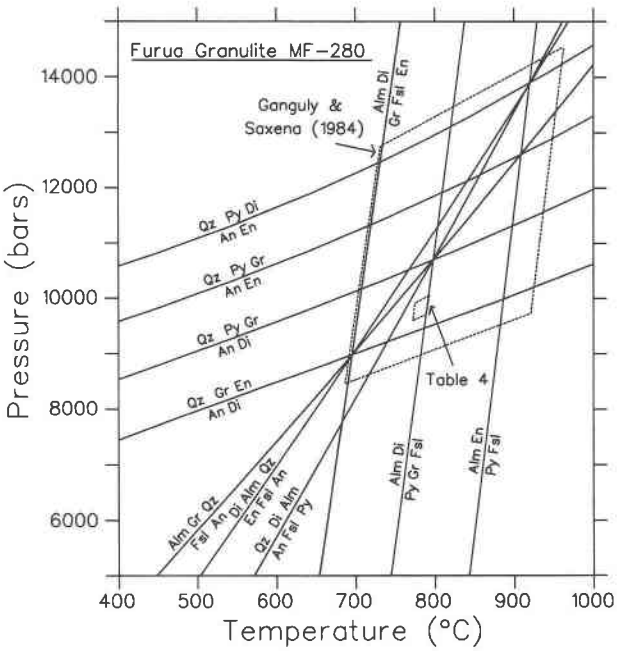

Fig. 12. Calculated stable and metastable equilibria involving garnet, plagioclase, orthopyroxene, clinopyroxene, and quartz for granulite MF-280 of Coolen (1980). Plotted equilibria were calculated with standard-state thermodynamic data from Table 3 and from Berman (1988) using the garnet mixing model of Moecher et al. (1988). Dotted outlined areas show the range of the same intersections produced with the garnet mixing models of Ganguly and Saxena (1984) and of Table 4. Note the marked reduction in scatter between, and generally lower pressure, of the *P-T* intersections calculated with the garnet mixing properties in Table 4.

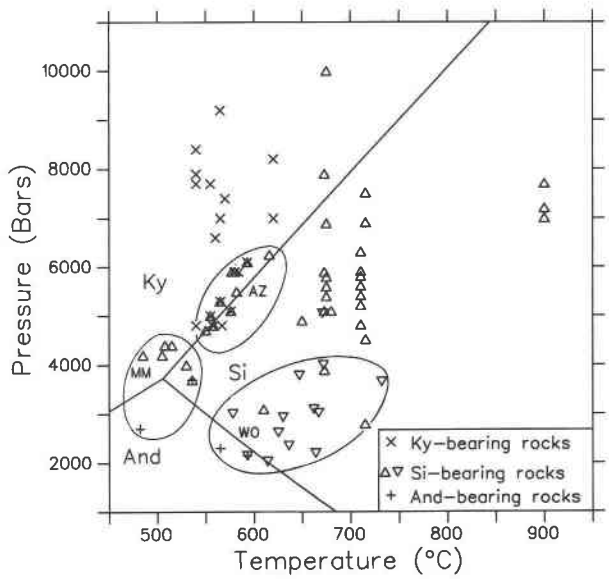

Fig. 13. Comparison of the calculated Al-silicate phase diagram with pressures computed from Equilibrium A using the garnet mixing properties in Table 4 and standard-state thermodynamic data of Berman (1988). With the exception of circled data, samples are the same as those used by Newton and Haselton (1981), with their average temperature estimates. Circled fields are for rocks from Mount Moosilauke (Hodges and Spear, 1982), Azure Lake (Pigage, 1982), and Wopmay orogen (triangles, St. Onge, 1984) that contain more than one Al-silicate polymorph. For these samples, plotted *P-T* locations represent intersections of Equilibrium A with the formulation of the garnet-biotite thermometer discussed in the text.

number of standard-state properties are involved in the calculation, and these are extremely well constrained by both direct calorimetric measurements as well as phase-equilibrium data. The major sources of uncertainty in using this test to assess garnet solution properties are the effects of uncertainties in standard-state properties and plagioclase solution properties. Although Berman (1988) does not present uncertainties in standard-state properties, pressures computed with Equilibrium A are viewed more optimistically than concluded by Hodges and McKenna (1987), because the process of thermodynamic analysis results in significant refinement beyond the experimental data concerned solely with this equilibrium. As pointed out by Hodges and McKenna (1987), the effects of uncertainties in plagioclase solution properties cannot be quantified because of the variety of different assumptions that form the basis of alternate model calibrations. An additional source of error is the nontrivial shift in the position of the Al-silicate phase boundaries for any given rock caused by grain size and minor impurities (e.g., Kerrick, 1987). Because the slope of the kyanite-sillimanite transition is almost parallel to that of equilibrium A, errors in estimated equilibration temperatures of the rock are of importance only in comparison with andalusite-sillimanite assemblages.

Use of the standard-state properties provided by Berman (1988) and the garnet solution properties in Table 4 leads to good agreement between pressures computed with Equilibrium A and the calculated Al-silicate phase diagram (Fig. 13). As with the calibration of Newton and Haselton (1981), the only major discrepancy occurs for a sillimanite-bearing granulite (calculated pressure = 10.0 kbar) reported by Perkins (1979), but much of this discrepancy may be due to errors in the computed anorthite activity, as this sample contains the most anorthite-poor plagioclase (X_{An} = 0.05) of all the samples plotted. The remaining small inconsistencies are within the uncertainty of the pressure comparison, and it is satisfying to find that such good agreement can be achieved without resort to the large ternary interaction parameters derived by Ganguly and Saxena (1984) through optimization of this same comparison.

A much more sensitive test than placing a given sample within one stability field can be applied to rocks that contain two or more Al-silicate polymorphs (Fig. 13). Although discrepancies are noted for individual Mount Moosilauke samples, these are consistent with the expected shifts in Al-silicate phase boundaries caused by

the partitioning of Mn into andalusite relative to sillimanite and sillimanite relative to kyanite. Low Mn pelites from Azure Lake containing kyanite and sillimanite fall within 0.5 kbar of this transition. Excellent agreement is also found with andalusite, andalusite-sillimanite, and sillimanite-bearing pelites from Wopmay orogen (St. Onge, 1984), with the andalusite-sillimanite sample plotting within 0.2 kbar of this phase transition.

The above comparisons of computed pressures for Al-silicate assemblages and garnet-biotite temperatures for Mn-rich samples suggest that the solution properties in Table 4 can be used reliably for geological applications with standard-state data from Table 3 and from Berman (1988). Nevertheless much additional work is required to refine these properties, especially excess entropies of mixing. Carefully reversed phase-equilibrium experiments that extend over a wider range of temperature would be a worthwhile complement to direct measurements of excess entropy. For the grossular-pyrope binary, experiments involving more Ca-rich compositions are required. Systematic volume measurements would also be helpful in defining excess volumes from the large amount of scatter among the data already gathered. Until such experimental data become available, careful analysis of data from natural assemblages can be expected to provide additional constraints that can be incorporated into future refinements of the garnet solution model derived in this paper.

Acknowledgments

I am very grateful to S. R. Bohlen, A. Koziol, R. C. Newton, and B. J. Wood for generously providing details of their experimental work prior to its publication. Thanks are also due to K. L. Currie, M. Engi, E. Froese, T. M. Gordon, A. M. Koziol, and J. L. Munoz for critical reviews and to D. McMullin for assisting with data analysis. Some financial support was provided through NSERC grant OGP0037234. This is Geological Survey of Canada contribution 20089.

References cited

Anderson, D.J., and Lindsley, D.H. (1981) A valid Margules formulation for an asymmetric ternary solution: Revision of the olivine-ilmenite thermometer, with applications. Geochimica et Cosmochimica Acta, 45, 847–853.

Anovitz, L.M., and Essene, E.J. (1987) Compatibility of geobarometers in the system CaO-FeO-Al_2O_3-SiO_2-TiO_2 (CFAST): Implications for garnet mixing models. Journal of Geology, 95, 633–645.

Berman, R.G. (1988) Internally-consistent thermodynamic data for stoichiometric minerals in the system Na_2O-K_2O-CaO-MgO-FeO-Fe_2O_3-Al_2O_3-SiO_2-TiO_2-H_2O-CO_2. Journal of Petrology, 29, 445–522.

Berman, R.G., and Brown, T.H. (1984) A thermodynamic model for multicomponent melts, with application to the system CaO-Al_2O_3-SiO_2. Geochimica et Cosmochimica Acta, 48, 661–678.

——— (1988) A general method for thermobarometric calculations, with a revised garnet solution model and geologic applications. Geological Society of America Abstracts with Programs, 20, A98.

Berman, R.G., Engi, M., Greenwood, H.J., and Brown, T.H. (1986) Derivation of internally consistent thermodynamic properties by the technique of mathematical programming, a review with application to the system MgO-SiO_2-H_2O. Journal of Petrology, 27, 1331–1364.

Bohlen, S.R., and Liotta, J.J. (1986) A barometer for garnet amphibolites and garnet granulites. Journal of Petrology, 27, 1025–1034.

Bohlen, S.R., Wall, V.J., and Boettcher, A.L. (1983a) Experimental investigations and geological applications of equilibria in the system FeO-TiO_2-Al_2O_3-SiO_2-H_2O. American Mineralogist, 68, 1049–1058.

——— (1983b) Experimental investigation and application of garnet granulite equilibria. Contributions to Mineralogy and Petrology, 83, 52–61.

Chatterjee, N.D., and Froese, E. (1975) A thermodynamic study of the pseudobinary join muscovite-paragonite in the system $KAlSi_3O_8$-$NaAlSi_3O_8$-Al_2O_3-SiO_2-H_2O. American Mineralogist, 60, 985–993.

Coolen, J.J.M. (1980) Chemical petrology of the Furua granulite complex, southern Tanzania. GUA (Amsterdam) Paper 13, 1–258.

Cressey, G., Schmid, R., and Wood, B.J. (1978) Thermodynamic properties of almandine-grossular garnet solid solutions. Contributions to Mineralogy and Petrology, 67, 397–404.

Davidson, P.M. and Lindsley, D.H. (1989) Thermodynamic analysis of pyroxene-olivine-quartz equilibria in the system CaO-MgO-FeO-SiO_2. American Mineralogist, 74, 18–30.

Davies, P.K., and Navrotsky, A. (1983) Quantitative correlations of deviations from ideality in binary and pseudobinary solid solutions. Journal of Solid State Chemistry, 46, 1–22.

Delaney, J.M. (1981) A spectral and thermodynamic investigation of synthetic pyrope-grossular garnets, 201 p. Ph.D. thesis, University of California, Los Angeles, California.

Engi, M., Berman, R.G., and Evans, B.W. (1984) A thermodynamic data base for minerals: II. The system SiO_2-MgO-Fe-C-H-O. Proceedings of the IUPAC Conference on Chemical Thermodynamics, paper 179.

Ferry, J.M., and Spear, F.S. (1978) Experimental calibration of partitioning of Fe and Mg between biotite and garnet. Contributions to Mineralogy and Petrology, 66, 113–117.

Fuhrman, M.L., and Lindsley, D.H. (1988) Ternary-feldspar modeling and thermometry. American Mineralogist, 73, 201–216.

Ganguly, J., and Kennedy, G.C. (1974) The energetics of natural garnet solid solution: I. Mixing of the aluminosilicate end-members. Contributions to Mineralogy and Petrology, 48, 137–148.

Ganguly, J., and Saxena, S.K. (1984) Mixing properties of aluminosilicate garnets: Constraints from natural and experimental data, and applications to geothermo-barometry. American Mineralogist, 69, 88–97.

Geiger, C.A., Newton, R.C., and Kleppa, O.J. (1987) Enthalpy of mixing of synthetic almandine-grossular and almandine-pyrope garnets from high-temperature solution calometry. Geochimica et Cosmochimica Acta, 51, 1755–1763.

Harley, S.L. (1984) An experimental study of the partitioning of Fe and Mg between garnet and orthopyroxene. Contributions to Mineralogy and Petrology, 86, 359–373.

Haselton, H.T., and Newton, R.C. (1980) Thermodynamics of pyrope-grossular garnets and their stabilities at high temperatures and pressures. Journal of Geophysical Research, 85, 6973–6982.

Haselton, H.T., and Westrum, E.F. (1980) Low temperature heat capacities of pyrope, grossular, and $pyrope_{60}grossular_{40}$. Geochimica et Cosmochimica Acta, 44, 701–709.

Hensen, B.J., Schmid, R., and Wood, B.J. (1975) Activity-composition relations for pyrope-grossular garnet. Contributions to Mineralogy and Petrology, 51, 161–166.

Hewitt, D.A., and Wones, D.R. (1975) Physical properties of some synthetic Fe-Mg-Al trioctahedral biotites. American Mineralogist, 60, 854–862.

Hodges, K.V., and McKenna, L.W. (1987) Realistic propagation of uncertainties in geologic thermobarometry. American Mineralogist, 72, 671–680.

Hodges, K.V., and Spear, F.S. (1982) Geothermometry, geobarometry and the Al_2SiO_5 triple point at Mt. Moosilauke, New Hampshire. American Mineralogist, 67, 1118–1134.

Indares, A., and Martingole, J. (1985) Biotite-garnet geothermometry in the granulite facies: The influence of Ti and Al in biotite. American Mineralogist, 70, 272–278.

Jackson, S.L. (1989) Extension of Wohl's ternary asymmetric solution model to 4 and n components. American Mineralogist, 74, 14–17.

Kawasaki, T., and Matsui, Y. (1983) Thermodynamic analyses of equilibria involving olivine, orthopyroxene, and garnet. Geochimica et Cosmochimica Acta, 47, 1661–1680.

Kerrick, D.M. (1987) Fibrolite in contact aureoles of Donegal, Ireland. American Mineralogist, 72, 240–255.

Kitayama, K., and Katsura, T. (1968) Activity measurements in ortho-

silicate and metasilicate solid solution: Mg_2SiO_4-$FeSiO_4$ and $MgSiO_3$-$FeSiO_3$ at 1204 C. Bulletin of the Chemical Society of Japan, 41, 1146–1151.

Koziol, A.M. (1988) Activity-composition relations of selected garnets determined by phase equilibrium experiments. Ph.D. thesis, University of Chicago, Chicago.

Koziol, A.M., and Newton, R.C. (1987) Experimental determination of spessartine-grossular solid solution relations. EOS, 68, 460.

——— (1988a) Redetermination of the anorthite breakdown reaction and improvement of the plagioclase-garnet-Al_2SiO_5 geobarometer. American Mineralogist, 73, 216–223.

——— (1988b) Experimental determination of almandine-grossular and (Ca,Fe,Mg) ternary garnet solid solution relations. EOS, 69, 498.

——— (1988c) The activity of grossular in ternary (Ca,Fe,Mg) garnet determined by reversed phase-equilibrium experiments at 1000 °C and 900 °C. Geological Society of America Abstracts with Programs, 20, A191.

Lee, H.Y., and Ganguly, J. (1988) Equilibrium compositions of coexisting garnet and orthopyroxene: Experimental determinations in the system FeO-MgO-Al_2O_3-SiO_2, and applications. Journal of Petrology, 29, 93–113.

Lindsley, D.H., Grover, J.E., and Davidson, P.M. (1981) The thermodynamics of the $Mg_2Si_2O_6$-$CaMgSi_2O_6$ join: A review and an improved model. In R.C. Newton, A. Navrotsky, and B.J. Wood, Eds., Thermodynamics of minerals and melts, p. 149–176. Springer-Verlag, New York.

Moecher, D.P., Essene, E.J., and Anovitz, L.M. (1988) Calculation and application of clinopyroxene-garnet-plagioclase-quartz geobarometers. Contributions to Mineralogy and Petrology, 100, 92–106.

Mueller, R.F. (1972) Stability of biotite: A discussion. American Mineralogist, 57, 300–317.

Newton, R.C. (1983) Geobarometry of high-grade metamorphic rocks. American Journal of Science, 283-A, 1–28.

Newton, R.C., and Haselton, H.T. (1981) Thermodynamics of the plagioclase-Al_2SiO_5-quartz geobarometer. In R.C. Newton, A. Navrotsky, and B.J. Wood, Eds., Thermodynamics of minerals and melts, p. 131–148. Springer-Verlag, New York.

Newton, R.C., and Perkins, D., III. (1982) Thermodynamic calibration of geobarometers based on the assemblages garnet-plagioclase-orthopyroxene (clinopyroxene)-quartz. American Mineralogist, 67, 203–222.

Newton, R.C., Charlu, T.V., and Kleppa, O.J. (1977) Thermochemistry of high pressure garnets and clinopyroxenes in the system CaO-MgO-Al_2O_3-SiO_2. Geochimica et Cosmochimica Acta, 41, 369–377.

Perkins, D. III (1979) Application of new thermodynamic data to mineral equilibria. Ph.D. thesis, University of Michigan, Ann Arbor, Michigan.

Perkins, D., III, and Chipera, S.J. (1985) Garnet-orthopyroxene-plagioclase-quartz barometry: Refinement and application to the English River subprovince and Minnesota River valley. Contributions to Mineralogy and Petrology, 89, 69–80.

Peterson, J.W., and Newton, R.C. (1988) Experimental *P-T* constraints on the phlogopite-quartz-sanidine-enstatite–vapor-liquid invariant point. Geological Society of America Abstracts with Programs, 20, A190.

Pigage, L.C. (1982) Linear regression analysis of sillimanite-forming reactions at Azure Lake, British Columbia. Canadian Mineralogist, 20, 349–378.

Powell, R., and Holland, T.J.B. (1988) An internally consistent dataset with uncertainties and correlations: 3. Applications to geobarometry, worked examples and a computer program: Journal of Metamorphic Geology, 6, 173–204.

Raeside, R.P., Hill, J.D., and Eddy, B.G. (1988) Metamorphism of Meguma group metasedimentary rocks, Whitehead Harbour area, Guysborough County, Nova Scotia. Maritime Sediments and Atlantic Geology, 24, 1–9.

Sack, R.O., and Ghiorso, M.S. (1989) Importance of considerations of mixing properties in establishing an internally consistent thermodynamic database: Thermochemistry of minerals in the system Mg_2SiO_4-Fe_2SiO_4-SiO_2. Contributions to Mineralogy and Petrology, 102, 41–68.

Sakawa, M., Whiteway, S.G., and Masson, C.R. (1978) Activity of FeO in the ternary system SiO_2-MgO-FeO and constitution of SiO_2. Transactions of the Iron and Steel Institute of Japan, 18, 173–176.

Saxena, S.K., and Chatterjee, N. (1986) Thermochemical data on mineral phases: The system CaO-MgO-Al_2O_3-SiO_2. Journal of Petrology, 27, 827–842.

Sharma, K.C., Agrawal, R.D., and Kapoor, M.L. (1987) Determination of thermodynamic properties of (Fe,Mg)-pyroxenes at 1000 K by the emf method. Earth and Planetary Science Letters, 85, 302–310.

St. Onge, M.R. (1984) Geothermometry and geobarometry in pelitic rocks of north-central Wopmay orogen (early Proterozoic), Northwest Territories, Canada. Geological Society of America Bulletin, 95, 196–208.

Wohl, K. (1946) Thermodynamic evaluation of binary and ternary liquid systems. Transactions of the American Institute of Chemical Engineers, 42, 215–249.

——— (1953) Thermodynamic evaluation of binary and ternary liquid systems. Chemical Engineering Progress, 49, 218–219.

Wones, D.R., and Eugster, H.P. (1965) Stability of biotite: Experiment, theory, and application. American Mineralogist, 50, 1228–1272.

Wood, B.J. (1976) The reaction phlogopite + quartz = enstatite + sanidine + H_2O. Progress in Experimental Petrology, 11, 17–19.

——— (1987) Thermodynamics of multicomponent systems containing several solid solutions. In Mineralogical Society of America Reviews in Mineralogy, 17, 71–96.

——— (1988) Activity measurements and excess entropy-volume relationships for pyrope-grossular garnets. Journal of Geology, 96, 721–729.

Wood, B.J., and Banno, S. (1973) Garnet-orthopyroxene and orthopyroxene-clinopyroxene relationships in simple and complex systems. Contributions to Mineralogy and Petrology, 42, 109–124.

Woodland, A.B., and Wood, B.J. (1989) Electrochemical measurement of the free energy of almandine ($Fe_3Al_2Si_3O_{12}$) garnet. Geochimica et Cosmochimica Acta, 53, 2277–2282.

Manuscript received April 7, 1989
Manuscript accepted November 22, 1989

Appendix 1

The equations below can be used for the calculation of activities in the grossular-pyrope-almandine-spessartine system using Margules parameters from Table 4.

Expansion of Equation 1 yields (1 = grossular, 2 = pyrope, 3 = almandine, 4 = spessartine):

$$\begin{aligned}3RT \ln \gamma_{Gr} = {} & W_{112}(2X_1X_2 - 2X_1^2X_2) + W_{122}(X_2^2 - 2X_1X_2^2) \\ & + W_{113}(2X_1X_3 - 2X_1^2X_3) + W_{133}(X_3^2 - 2X_1X_3^2) \\ & + W_{114}(2X_1X_4 - 2X_1^2X_4) + W_{144}(X_4^2 - 2X_1X_4^2) \\ & + W_{223}(-2X_2^2X_3) + W_{233}(-2X_2X_3^2) \\ & + W_{224}(-2X_2^2X_4) + W_{244}(-2X_2X_4^2) \\ & + W_{334}(-2X_3^2X_4) + W_{344}(-2X_3X_4^2) \\ & + W_{123}(X_2X_3 - 2X_1X_2X_3) + W_{124}(X_2X_4 - 2X_1X_2X_4) \\ & + W_{134}(X_3X_4 - 2X_1X_3X_4) + W_{234}(-2X_2X_3X_4)\end{aligned} \tag{A1}$$

$$\begin{aligned}3RT \ln \gamma_{Py} = {} & W_{112}(X_1^2 - 2X_1^2X_2) + W_{122}(2X_1X_2 - 2X_1X_2^2) \\ & + W_{113}(-2X_1^2X_3) + W_{133}(-2X_1X_3^2) \\ & + W_{114}(-2X_1^2X_4) + W_{144}(-2X_1X_4^2) \\ & + W_{223}(2X_2X_3 - 2X_2^2X_3) + W_{233}(X_3^2 - 2X_2X_3^2) \\ & + W_{224}(2X_2X_4 - 2X_2^2X_4) + W_{244}(X_4^2 - 2X_2X_4^2) \\ & + W_{334}(-2X_3^2X_4) + W_{344}(-2X_3X_4^2) \\ & + W_{123}(X_1X_3 - 2X_1X_2X_3) + W_{124}(X_1X_4 - 2X_1X_2X_4) \\ & + W_{134}(-2X_1X_3X_4) + W_{234}(X_3X_4 - 2X_2X_3X_4)\end{aligned} \tag{A2}$$

$$
\begin{aligned}
3RT \ln \gamma_{Alm} &= W_{112}(-2X_1^2X_2) + W_{122}(-2X_1X_2^2) \\
&+ W_{113}(X_1^2 - 2X_1^2X_3) + W_{133}(2X_1X_3 - 2X_1X_3^2) \\
&+ W_{114}(-2X_1^2X_4) + W_{144}(-2X_1X_4^2) \\
&+ W_{223}(X_2^2 - 2X_2^2X_3) + W_{233}(2X_2X_3 - 2X_2X_3^2) \qquad \text{(A3)} \\
&+ W_{224}(-2X_2^2X_4) + W_{244}(-2X_2X_4^2) \\
&+ W_{334}(2X_3X_4 - 2X_3^2X_4) + W_{344}(X_4^2 - 2X_3X_4^2) \\
&+ W_{123}(X_1X_2 - 2X_1X_2X_3) + W_{124}(-2X_1X_2X_4) \\
&+ W_{134}(X_1X_4 - 2X_1X_3X_4) + W_{234}(X_2X_4 - 2X_2X_3X_4)
\end{aligned}
$$

$$
\begin{aligned}
3RT \ln \gamma_{Sp} &= W_{112}(-2X_1^2X_2) + W_{122}(-2X_1X_2^2) \\
&+ W_{113}(-2X_1^2X_3) + W_{133}(-2X_1X_3^2) \\
&+ W_{114}(X_1^2 - 2X_1^2X_4) + W_{144}(2X_1X_4 - 2X_1X_4^2) \\
&+ W_{223}(-2X_2^2X_3) + W_{233}(-2X_2X_3^2) \qquad \text{(A4)} \\
&+ W_{224}(X_2^2 - 2X_2^2X_4) + W_{244}(2X_2X_4 - 2X_2X_4^2) \\
&+ W_{334}(X_3^2 - 2X_3^2X_4) + W_{344}(2X_3X_4 - 2X_3X_4^2) \\
&+ W_{123}(-2X_1X_2X_3) + W_{124}(X_1X_2 - 2X_1X_2X_4) \\
&+ W_{134}(X_1X_3 - 2X_1X_3X_4) + W_{234}(X_2X_3 - 2X_2X_3X_4)
\end{aligned}
$$

with ternary parameters given by Equation 2. Activities are computed by

$$
\begin{aligned}
a_{Gr} &= (X_{Gr} \cdot \gamma_{Gr})^3 \\
a_{Py} &= (X_{Py} \cdot \gamma_{Py})^3 \\
a_{Alm} &= (X_{Alm} \cdot \gamma_{Alm})^3 \\
a_{Sp} &= (X_{Sp} \cdot \gamma_{Sp})^3
\end{aligned}
$$

Appendix 2

Abbreviations of mineral names:

Alm	=	almandine
An	=	anorthite
Ann	=	annite
En	=	enstatite
Fa	=	fayalite
Fs	=	ferrosilite
Gr	=	grossular
Ilm	=	ilmenite
Ky	=	kyanite
Ms	=	muscovite
Phl	=	phlogopite
Py	=	pyrope
Qz	=	quartz
Rt	=	rutile
Si	=	sillimanite
Sp	=	spessartine